International Journal of Smart Grid and Clean Energy

ADALINE based efficient voltage stabilization with variable balanced and unbalanced loads in microgrid

A. Elnady [a,b]

[a] *University of Sharjah, Sharjah, United Arab Emirates*
[b] *Adjunct- Royal Military College Kingston, Ontario, Canada*

Abstract

This paper presents an accurate tool for tracking the voltage unbalance in the microgrid. This accurate tracking depends on a new formulation of the adaptive linear neuron (ADALINE). This formulation has accurate estimation/extraction of positive-, negative-, and zero-sequence voltages. The paper introduces a control scheme that stabilizes the voltages at the loads side by adjusting the positive voltage around 1 pu and mitigating the negative-sequence voltage. This voltage stabilization is done through the developed control scheme, which has a cascaded-loop structure for voltage and current control. The control scheme along with the suggested estimation tool gives accurate results for stabilizing the voltage at the loads side for different loading conditions.

Keywords: ADALINE, voltage unbalance, balanced loads, unbalanced loads, control scheme, microgrid.

1. Introduction

The microgrid is a new technology and concept introduced to the distribution systems. The microgrid is introduced to substitute the small distribution systems with the concept of dispersed energy resources for diverse power flows. The microgrid is attributed with some merits such as low carbon emission, more reliability, less power loss, and diverse power sources. It is independent of the central power grid; meaning that it can be operated in a grid-connected mode or in a standalone mode [1-4].

Voltage unbalance is a common power quality problem in any power grid [5]. The voltage unbalance appears in the power system because of the unsymmetrical distribution of loads among the three-phase supply. The voltage unbalance including a change in positive-sequence voltages, existence of negative-sequence and zero-sequence voltages. The existence of the negative-sequence voltage in the power grid is dangerous because it increases the fluxing level in machines such as transformers and generators, which increases the saturation and causes more temperature rise [5-7]. The zero-sequence voltage also increases the fluxing level in machines, which increments the saturation. The mitigation of the zero-sequence voltage can be done by the connections of the transformer windings and generator windings. Therefore, the mitigation of the zero-sequence voltage is not necessarily included in the control scheme, but it rather can be mitigated using the system connection with the ground network. Meanwhile, the mitigation of the negative-sequence voltage is required to be included in the operational/control scheme of the microgrid.

The unbalance in the microgrid is still a new topic for research because the unique features of the microgrids [8-12]. The grounding system of the microgrid influences the unbalance in the microgrid. The grounding method is properly selected such that it can control the ground fault currents. Therefore, the common scheme of grounding is to connect the ground to the neutral wire at one point or at several points through an impedance (resistor and reactor) [9], [10]. From the load perspective, the existence of the grounded neutral at the load side is imperative, where this connection triggers the existence of zero-sequence components at the load side. It is noteworthy mentioning that the common transformer connections in microgrids are Yg/Δ and Yg/Yg [8].

Mitigation of the voltage unbalance entails the extraction of the unbalance components (positive-sequence voltage, negative-sequence voltage, and zero-sequence voltage). It is customary to mitigate the voltage unbalance by using custom power devices in the power grid. The mitigation process starts with

* Manuscript received September 16, 2019; revised August 28, 2020 .
Corresponding author. *E-mail address*: ayelnady71@gmail.com.
doi: 10.12720/sgce.9.5.872-878

unbalance extraction/tracking and then a control signal is generated to operate these custom power devices such as a dynamic voltage restorer (DVR) [13], distribution static compensator (DSTATCOM) [14], and unified power quality conditioner (UPQC) [15]. These publications focus on the mitigation of the negative-sequence components using these custom power devices.

The mitigation of the unbalance is still a problem under investigation because the custom power devices are not considered as an economical solution in the microgrid. The contribution of this research is articulated in three main points. Firstly, the mitigation of voltage unbalance is integrated in the control scheme. Secondly, there is no need for any mitigation device to eliminate the voltage unbalance. The utilized power sources (inverters) can be operated and controlled to cancel the unsymmetrical components. Lastly, the unbalance components are accurately estimated using a new formulation for ADALINE. This paper consists of four sections. The second section demonstrates the proposed control scheme. The third section shows the simulation results for stabilizing the voltages at different loads. The findings of this paper are concluded in the last.

2. Proposed Structure of Control Scheme

This section pinpoints the contribution of this research for stabilizing the voltage across the loads side. This section shows the configuration of the microgrid under study, the proposed control scheme to stabilize the voltage at loads, and the new formulation of ADALINE to estimate sequence voltages.

2.1 Configuration of microgrid

The aim of the suggested control scheme is to stabilize the voltage at loads bus (PCC) in the microgrid. This suggested scheme is developed based on the microgrid given in Fig. 1. This microgrid has several (three) inverters, which are connected to the PV system charging batteries. The inverters are located at one side and the loads are dispersed and connected to the PCC in the microgrid. The most important parameters for this microgrid are listed as $V_{PCC} = 6.6\ kV$, $S_{Tr1} = S_{Tr2} = 2.5MVA$, $Tr_1\ turn's\ ratio = 1.32 : 6.6\,kV$, $Tr_2\ turn's\ ratio = 6.6 : 0.4\,kV$, $Z_{feeder} = 1.2\Omega + 1.5\,j\,\Omega$.

2.2 Structure of control scheme

The suggested control scheme has two cascaded control loops (primary and secondary loops). The secondary control adjusts the voltage across the loads bus (PCC), and its output gives a current reference to the primary loop. Whereas, the primary loop controls the current that is injected by the inverters. Its output is the required injected voltage by inverters such that the load voltage is stabilized regardless any variation at loads. For the secondary voltage control loop, the reference voltage (input of this loop) is related to its reference current (output of this loop) by the impedance of the loads. The voltage and current references are expressed in the *d-q* rotating frame as,

$$V^{+-}_{load-d-ref} = I^{+-}_{load-d-ref} Z^{+-}_{loads}, V^{+-}_{load-q-ref} = I^{+-}_{load-q-ref} Z^{+-}_{loads} \tag{1}$$

The formula given in (1) looks linear; therefore, its controller can be a PI controller to give a satisfactory performance. For the primary control loop, the current reference is related to the injected voltage based on the configuration of the microgrid illustrated in Fig. 1. Its mathematical formulas for positive- and negative-sequences are given as,

$$\begin{aligned} E^{+}_{inv-d} &= V^{+}_{PCC-d} + RI^{+}_{inj-d} - \omega LI^{+}_{inj-q} + L\frac{dI^{+}_{inj-d}}{dt},\ E^{+}_{inv-q} = V^{+}_{PCC-q} + RI^{+}_{inj-q} + \omega LI^{+}_{inj-d} + L\frac{dI^{+}_{inj-q}}{dt} \\ E^{-}_{inv-d} &= V^{-}_{PCC-d} + RI^{-}_{inj-d} + \omega LI^{-}_{inj-q} + L\frac{dI^{-}_{inj-d}}{dt},\ E^{-}_{inj-q} = V^{-}_{PCC-q} + RI^{-}_{inj-q} - \omega LI^{-}_{inj-d} + L\frac{dI^{-}_{inj-q}}{dt} \end{aligned} \tag{2}$$

where L and R are the inductance and resistance of the feeder respectively, E_{inv} is the voltage at inverters' bus, and V_{PCC} is the voltage at loads bus. The mathematical formulation for the primary control loop can be linearized around its general operating condition by another PI controller. A control scheme is developed based on these cascaded loops. This suggested control scheme is depicted in Fig. 2.

2.3 Estimation of sequence components

The contribution in this research is exemplified in the new formulation of the adaptive linear neuron (ADALINE). The presented formulation differs from what is published in [16] in terms of the simplicity of ADALINE formulation. The ADALINE, in [16], depends on matrix forms and it is used in the *d-q* rotating frame. In [17], a multilayer feedforward neutral network used to extract the symmetrical components precludes its practical implementation. The multioutput-ADALINE and complex-ADALINE are used to estimate the symmetrical voltage components in [18] and [19] respectively, where their formulation is based on matrix equations, which require more time for their mathematical processes. The developed formulation in this research starts with defining any voltage in an exponential form as,

$$V = V^{+}e^{j\omega t} + V^{-}e^{-j\omega t} \tag{3}$$

The magnitudes V^{+} and V^{-} are defined in a complex vector form as,

$$V^{+} = a^{+}\angle\varphi^{+} = a^{+}e^{j\varphi^{+}},\ V^{-} = a^{-}\angle\varphi^{-} = a^{-}e^{j\varphi-} \tag{4}$$

Substituting (4) in (3) leads to

$$\begin{aligned} V &= a^{+}e^{j(\omega t+\varphi^{+})} + a^{-}e^{-j(\omega t-\varphi-)} \\ V &= a^{+}[\cos(\omega t+\varphi^{+}) + j\sin(\omega t+\varphi^{+})] + a^{-}[\cos(\omega t-\varphi^{-}) - j\sin(\omega t-\varphi^{-})] \\ V &= [a^{+}\cos(\omega t+\varphi^{+}) + a^{-}\cos(\omega t-\varphi^{-})] + j[a^{+}\sin(\omega t+\varphi^{+}) - a^{-}\sin(\omega t-\varphi^{-})] \end{aligned} \tag{5}$$

The expression in (5) is used to extract the voltage parameters. The real component of the voltage in (5) can be used to estimate the voltage parameters and it is expressed as,

$$V_{real} = [-a^{+}\sin\varphi^{+} + a^{-}\sin\varphi^{-}]\sin(\omega t) + [a^{+}\cos\varphi^{+} + a^{-}\cos\varphi^{-}]\cos(\omega t) \tag{6}$$

Equation (6) can be rewritten in a vector form as,

$$V_{real} = [-a^{+}\sin\varphi^{+}\quad a^{+}\cos\varphi^{+}\quad a^{-}\sin\varphi^{-}\quad a^{-}\cos\varphi^{-}] * [\sin(\omega t)\quad \cos(\omega t)\quad \sin(\omega t)\quad \cos(\omega t)]^{T} \tag{7}$$

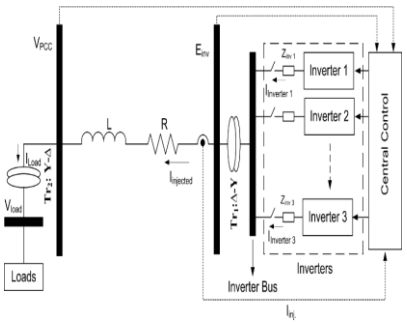

Fig. 1. Microgrid under study

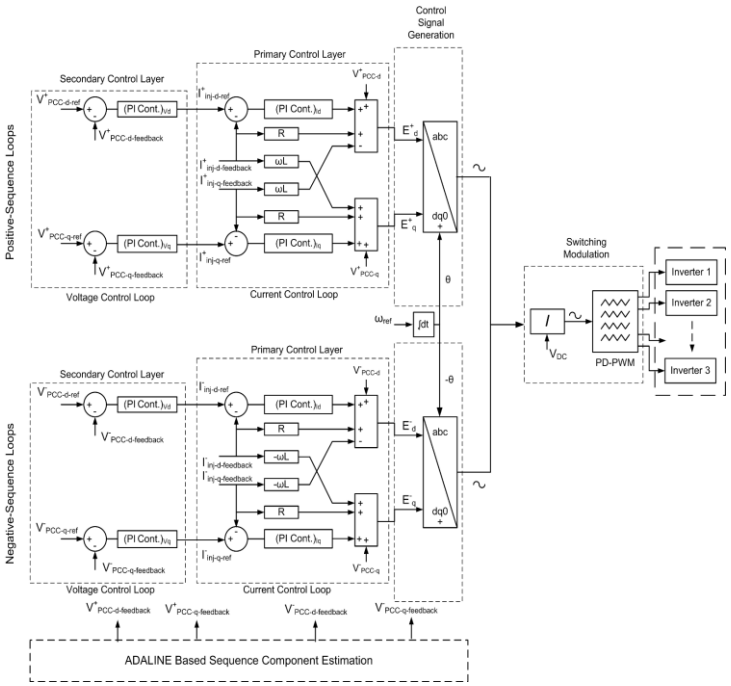

Fig. 2. Proposed control scheme

Based on the formula given written in (7), the phase-a voltage is expressed in a state-space form as,

$$\begin{aligned} V_{ph-a} &= W_{ph} * X_{ph-a} \\ W_{ph} &= [-a^{+}_{ph}\sin\varphi^{+}_{ph} \quad a^{+}_{ph}\cos\varphi^{+}_{ph} \quad a^{-}_{ph}\sin\varphi^{-}_{ph} \quad a^{-}_{ph}\cos\varphi^{-}_{ph}] \\ X_{ph-a} &= [\sin(2\pi 50k\Delta t) \quad \cos(2\pi 50k\Delta t) \quad \sin(2\pi 50k\Delta t) \quad \cos(2\pi 50k\Delta t)]^{T} \end{aligned} \tag{8}$$

where $\omega = 2\pi 50$, Δt is the sampling time, and k is the counter for the iterative process. Similarly, the phase-b voltage is expressed as,

$$\begin{aligned} V_{ph-b} &= W_{ph} * X_{ph-b} \\ W_{ph} &= [-a^{+}_{ph}\sin\varphi^{+}_{ph} \quad a^{+}_{ph}\cos\varphi^{+}_{ph} \quad a^{-}_{ph}\sin\varphi^{-}_{ph} \quad a^{-}_{ph}\cos\varphi^{-}_{ph}] \\ X_{ph-b} &= [\sin(2\pi 50k\Delta t - 2pi/3)\cos(2\pi 50k\Delta t - 2pi/3)\sin(2\pi 50k\Delta t + 2pi/3)\cos(2\pi 50k\Delta t + 2pi/3)]^{T} \end{aligned} \tag{9}$$

The phase-c voltage is also formulated as,

$$\begin{aligned} V_{ph-c} &= W_{ph} * X_{ph-c} \\ W_{ph} &= [-a^{+}_{ph}\sin\varphi^{+}_{ph} \quad a^{+}_{ph}\cos\varphi^{+}_{ph} \quad a^{-}_{ph}\sin\varphi^{-}_{ph} \quad a^{-}_{ph}\cos\varphi^{-}_{ph}] \\ X_{ph-c} &= [\sin(2\pi 50k\Delta t + 2pi/3)\cos(2\pi 50k\Delta t + 2pi/3)\sin(2\pi 50k\Delta t - 2pi/3)\cos(2\pi 50k\Delta t - 2pi/3)]^{T} \end{aligned} \tag{10}$$

The state space formulas for the three-phase voltages are given in (8) to (10). This state-space formulation is recursively calculated by their implementation in the ADALINE algorithm. This algorithm calculates the error as,

$$\begin{aligned} e_{ph-a} &= V_{PCC-a} - \left(\frac{V_{PCC-a} + V_{PCC-b} + V_{PCC-c}}{3}\right) - W_{ph}X_{ph-a} \\ e_{ph-b} &= V_{PCC-b} - \left(\frac{V_{PCC-a} + V_{PCC-b} + V_{PCC-c}}{3}\right) - W_{ph}X_{ph-b} \\ e_{ph-c} &= V_{PCC-c} - \left(\frac{V_{PCC-a} + V_{PCC-b} + V_{PCC-c}}{3}\right) - W_{ph}X_{ph-c} \end{aligned} \tag{11}$$

The change in the coefficients W is dictated by the Widrow-Hoff learning rule as [20],

$$\begin{aligned} \Delta W_{ph-a}(k) &= \eta e_{ph-a}X_{ph-a} / (X^{T}_{ph-a} * X_{ph-a}), \\ \Delta W_{ph-b}(k) &= \eta e_{ph-b}X_{ph-b} / (X^{T}_{ph-b} * X_{ph-b}) \\ \Delta W_{ph-c}(k) &= \eta e_{ph-c}X_{ph-c} / (X^{T}_{ph-c} * X_{ph-c}) \end{aligned} \tag{12}$$

The updated coefficients $W(k+1)$ are written as [20],

$$\begin{aligned} &W_{ph-updated1}(k) = \Delta W_{ph-a}(k) + W_{ph}(k), W_{ph-updated2}(k) = \Delta W_{ph-b}(k) + W_{ph-updated1}(k) \\ &W_{ph-updated3}(k) = \Delta W_{ph-c}(k) + W_{ph-updated2}(k), W_{ph}(k+1) = W_{ph-updated3}(k) \end{aligned} \tag{13}$$

Equations (12) to (14) go in an iterative loop to have online tracking for unbalance components. The instantaneous positive-sequence, negative-sequence, and zero-sequence voltages are given as,

$$\begin{aligned} V_a(t)_{positive} &= W_{ph}(1)X_{ph-a}(1) + W_{ph}(2)X_{ph-a}(2) \\ V_a(t)_{negative} &= W_{ph}(3)X_{ph-a}(3) + W_{ph}(4)X_{ph-a}(4) \\ V_a(t)_{zero} &= (V_a(t) - V_a(t)_{positive} - V_a(t)_{negative}) \end{aligned} \tag{14}$$

The magnitude and angle of any-sequence voltage are calculated as,

$$Mag = \sqrt{W_{ph}^{2}(i) + W_{ph}^{2}(i+1)}, \quad angle = \tan^{-1}(W_{ph}(i) / W_{ph}(i+1)) \rightarrow i = 1 \ or \ 3 \tag{15}$$

Eventually, the formulas in (14) and (15) are used to estimate the positive-sequence and negative-sequence voltages at the loads side (PCC) to complete the operation of the control scheme in Fig. 2.

3. Simulation Results

This section shows the simulation results for the proposed estimation and control scheme of Fig. 2.

3.1 Performance of Control Scheme for Balanced Loads

The loads in the microgrid are a parallel combination for two balanced loads of $Z_{load1} = 55 + 18.84j$ and $Z_{load2} = 65 + 31.4j$ for the time duration from 0 to 3 s. At time t = 3 s, the second load Z_{load2} is disconnected. The zero-sequence voltage is blocked by the transformer connection shown in Fig. 1. There are several factors used to express the voltage unbalance across the loads. Important factors are the positive-sequence factor (VUF^{+}) and negative-sequence factor (VUF^{-}) written as,

$$VUF^{+} = \frac{positive-sequence\ voltage}{rated\ typical\ phase\ voltage}, VUF^{-} = \frac{negative-sequence\ voltage}{positive-sequence\ voltage} \tag{16}$$

For balanced loads, the positive-sequence voltage control is the functional loop since the loads are balanced and the negative-sequence voltage is almost neglected. The reference voltages in the d-q frame are $V_{PCC-d-ref}^{+} = 5400V$ and $V_{PCC-q-ref}^{+} = 0V$. These values are selected to have $6.6kV$ balanced line voltages at the PCC in Fig. 1. The control scheme of Fig. 2 needs feedback voltage at the PCC, $V_{PCC-d-feedback}^{+}$ and $V_{PCC-q-feedback}^{+}$, which are estimated using the developed formulation in (12-15). The positive-sequence factor is displayed in Fig. 3, where it shows almost 100% and the negative-sequence factor is almost 1%. The instantaneous voltages for the 1st and 2nd balanced loads are portrayed in Fig. 4.

3.2 Performance of control scheme for unbalanced loads

The unbalance loads are connected at time t = 6. At this time, the microgrid has a parallel combination for balanced loads of $Z_{load1} = 55 + 18.84j$ and unbalanced loads of $Z_{ph-a} = 25 + 6.28j$, $Z_{ph-b} = 50 + 31.4j$, and $Z_{ph-c} = 35 + 15.7j$ for the time range from t = 6 s till t = 9 s. Afterwards, more unbalanced loads are connected to the microgrid with impedances of $Z_{ph-a} = 30 + 9.42j$, $Z_{ph-b} = 35 + 11j$, and $Z_{ph-c} = 45 + 14.13j$ for the time duration from 9 s to 12 s. In order to eliminate the negative-sequence voltage, the references voltage are $V_{PCC-d-ref}^{-} = 0V$ and $V_{PCC-q-ref}^{-} = 0V$. The feedback voltages are estimated using the formula given in (12-15). The negative factor defined in (16) is presented in Fig. 5-a, without the negative-sequence control, which indicates that the negative factor is almost 4%, which is considered above the permissible limit (2%) based on IEEE standard 1159-1995. The instantaneous estimation of the positive-sequence and negative-sequence voltages by the presented formulation of ADALINE is displayed in Fig. 5-b.

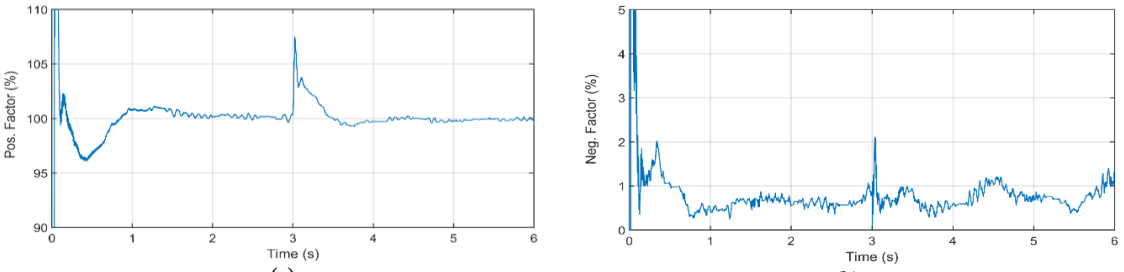

(a) (b)

Fig. 3. Performance of control scheme for variable balanced loads (a) Positive factor (b) Negative factor

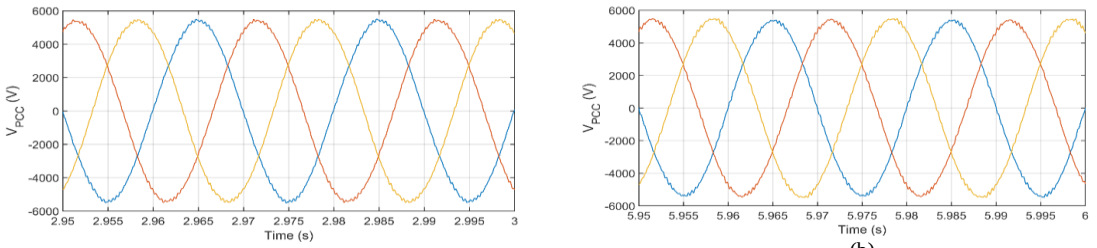

(a) (b)

Fig. 4. Instantaneous three-phase voltages across variable balanced loads (a) Voltage waveforms at PCC for 1st balanced loads (b) Voltage waveforms at PCC for 2nd balanced loads

The instantaneous three-phase voltages at the PCC without the activation of the negative-sequence control loop is given in Fig. 5-c.

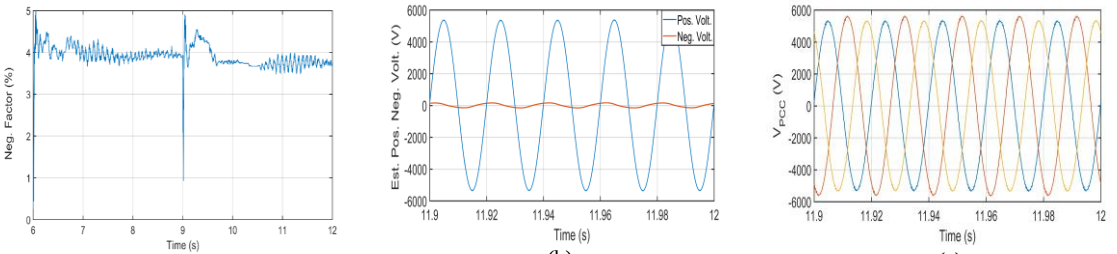

(a) (b) (c)

Fig. 5. Performance of control scheme without activation of negative-sequence control (a) Negative factor (b) Estimated instantaneous positive and negative sequence voltages (c) Instantaneous voltage waveforms at PCC

The effectiveness of the proposed whole control scheme for voltage stabilization across the unbalanced loads is justified by the sequence factors in Fig. 6-a and Fig. 6-b and by the instantaneous three-phase voltage waveforms at the PCC in Fig. 6-c. Comparing Fig. 5-a to Fig. 6-a and Fig. 5-c to Fig. 6-c indicates much improvement in stabilizing the positive-sequence voltage and also much reduction in the negative-sequence voltage to be less than 2%, and it also justifies the voltage waveforms in Fig. 6-c.

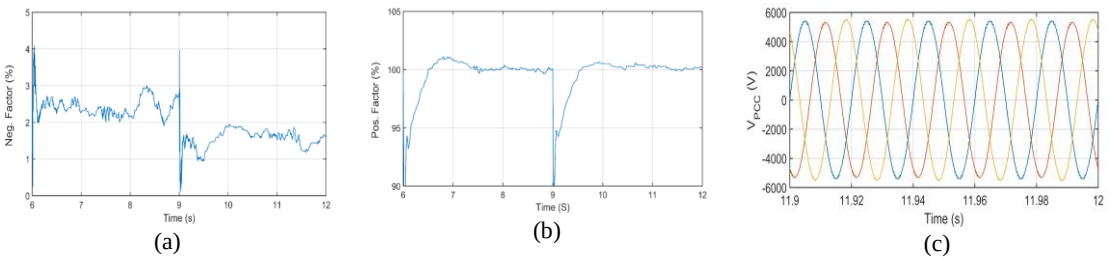

(a) (b) (c)

Fig. 6. Performance of whole control scheme including positive and negative control (a) Negative factor (b) Positive factor (c) Instantaneous voltage waveforms at PCC

4. Conclusion

This paper propounds a control scheme that maintains the voltages constant across variable loads. This scheme is used to operate several inverters in the microgrid such that the positive-sequence voltage becomes stable around 1 pu and the negative-sequence voltage is at its minimum level. This presented control scheme needs positive and negative voltages, which are estimated using a simple formulation for ADALINE. The simulation results prove that the suggested operational/control scheme is efficient for stabilizing the voltage around 1 pu and mitigating the negative-sequence voltage to be less than 2%.

Conflict of Interest

The author declares no conflict of interest.

References

[1] IEEE Standard 2030.7-2017, IEEE Standard for Specifications of Microgrid Controller, [Online]. Available: https://standards.ieee.org/standard/2030_7-2017.html.
[2] IEEE Standard 1547.4-2011, IEEE Guide for Design, Operation, and Integration of Distributed Resource Island Systems with Electric Power Systems, [Online]. Available: https://ieeexplore.ieee.org/document/5960751/
[3] How Microgrids Work. [Online]. Available: https://www.energy.gov/articles/how-microgrids-work
[4] Kroposki B, Basso T, DeBlasio R. Microgrid standards and technologies. In: *Proc. of IEEE Power and Energy Society* General *Meeting*, 2008: 1-6.
[5] Jouanne A, Banerjee B. Assessment of voltage unbalance. *IEEE Trans. on Power Delivery*, 2001; 16(4): 782-790.
[6] Limits for Voltage Unbalance in the Electricity Supply System, (Technical Report) Abu Dhabi Distribution Company and Al Ain Distribution Company.
[7] Hochgraf C, Lasseter RH. Statcom controls for operation with unbalanced voltages. *IEEE Trans. on Power Delivery*, 1998; 13(2): 538-544.
[8] Johnson G, Schroeder M, Dalke G. A review of system grounding methods and zero sequence current sources. In: *Proc. of Annual Conference of Protective Relay Engineers*, TX-USA, 2008: 1-6.
[9] Mohammadi J, Ajaei F, Stevens G. AC microgrid grounding strategies. In: *Proc. of IEEE/IAS 54th Industrial and Commercial Power Systems Technical Conference*, Niagra Falls-ON-Canada, 2018: 1-6.
[10] Mohammadi J, Ajaei F, Stevens G. Grounding the AC microgrid. *IEEE Trans. on Industry Applications*, 2019; 55(1): 98-105.
[11] Souza WF, Severo-Mendes MA, Lopes LAC. Analysis of a microgrid with unbalanced load comparing three-phase and per-phase voltage droop control. In: *Proc. of 13th IEEE Brazilian Power Electronics Conference and 1st Southern Power Electronics Conference* (COBEP/SPEC), Fortaleza-Brazil, 2015: 1-5.
[12] Savaghebi M, Jalilian A, Vasquez JC, Guerrero JM. Secondary control scheme for voltage unbalance compensation in an islanded droop-controlled microgrid. *IEEE Trans. on Smart Grid*, 2012; 3(2): 797-807.
[13] Elnady A, Salama MMA. Mitigation of voltage disturbances using adaptive perceptron-based control algorithm. *IEEE Trans. on Power Delivery*, 2005; 20(1): 309-318.
[14] Elnady A, Salama MMA. Unified approach for mitigating voltage sag and voltage flicker using the DSTATCOM. *IEEE Trans. on Power Delivery*, 2005; 20(2): 992-1000.
[15] Ghosh A, Ledwich G. A unified power quality conditioner (UPQC) for simultaneous voltage and current compensation. *Electric Power System Research*, 2001; 59(1): 55-63.
[16] Abdeslam D, Wira P, Merckl é J. A new adaline approach for online voltage components extraction from unbalanced and perturbed power systems. In: *Proc. of 32th IEEE Annual Conference of the Industrial Electronics Society*, France, 2006: 1-6.
[17] Javier Alc ántara F, Salmer ón P. A new technique for unbalance current and voltage estimation with neural networks. *IEEE Trans. on Power Systems*, 2005; 20(2): 852-858.
[18] Marei MI, El-Saadany EF, Salama MMA. A processing unit for symmetrical components and harmonics estimation based on a new adaptive linear combiner structure. *IEEE Trans. on Power Delivery*, 2004; 19(3): 1245-1252.
[19] Shahroudi M, Abdollahzadeh H, Naderi MS, Mozafari B, Mahdavizadeh F, Tavighi A. Monitoring and unbalance mitigation of harmonic current symmetrical components, using double complex-ADALINE algorithm. In: *Proc. of 1st IEEE Power Quality* Conference, Tehran, Iran, 2010: 1-7.
[20] Widrow B, Lehr MA. 30 yaers of adaptive neural networks; perceptron, madaline and back propagation, In: *Proc. of IEEE*, 1990; 78(9):1415-1442.